On the circulation and water masses over the Antarctic continental slope and rise between 80 and 150°E

Nathaniel L. Bindoff[a,*], Mark A. Rosenberg[a], Mark J. Warner[b]

[a]*Antarctic Co-operative Research Centre, GPO Box 252-80, Hobart, Tasmania 7001, Australia*
[b]*School of Oceanography, University of Washington, Seattle, USA*

Abstract

The circulation and water masses in the region between 80 and 150°E and from the Antarctic continental shelf to the Southern Boundary of the Antarctic Circumpolar Current (ACC) (~ 62°S) are described from hydrographic and surface drifter data taken as part of the multi-disciplinary experiment, Baseline Research on Oceanography Krill and the Environment (BROKE). Two types of bottom water are identified, Adelie Land Bottom Water, formed locally between 140 and 150°E, and Ross Sea Bottom Water. Ross Sea Bottom Water is found only at 150°E, whereas Adelie Land Bottom Water is found throughout the survey region. The bottom water mass properties become progressively warmer and saltier to the west, suggesting a westward flow. All of the eight meridional CTD sections show an Antarctic Slope Front of varying strength and position with respect to the shelf break. In the water formation areas (between 140 and 150°E) and 104°E, the Antarctic Slope Front is more "V" shaped, while elsewhere it is one-sided. The shape of the slope front, and the presence or absence of water formation there, are consistent with other meridional sections in the Weddel Sea and simple theories of bottom-water formation (Gill, 1973. Deep-Sea Research 20, 111–140; Whitworth et al., 1998. In: Jacobs and Weiss (Eds.), Ocean, Ice and Atmosphere: Interactions at the Antartic Continental Margin, Antarctic Research Series. American Geophysical Union, Washington, pp. (1 − 27). ADCP surface velocities and buoy drift tracks show a strong westward flow over the shelf and slope regions. In the region 90–100°E there is a strong eastward flow of the waters just south of the Southern Boundary of the ACC, suggesting a recirculation of the westward slope current and the presence of a weak cyclonic gyre. Using the ADCP velocities as a reference for the CTD data, the average westward transport in this region is 29.4 ± 14.7 Sv. © 2000 Elsevier Science Ltd. All rights reserved.

* Corresponding author. Tel.: + 61-3-622-629-86; fax: + 61-3-622-629-73.
E-mail address: n.bindoff@utas.edu.au (N.L. Bindoff).

1. Introduction

Antarctica is surrounded by three broad-scale deep depressions. The Weddel-Enderby, Bellingshausen-Amundsen, and the Australian-Antarctic basins. This last basin is bounded on the west by Kerguelen Plateau and on the north and east by the South-Indian Rise. Unlike the two other basins, the Antarctic Coast in this sector has no major ice shelves and by comparison with the other two basins has a relatively narrow continental shelf. Bottom waters found in the Weddel-Enderby and Bellingshausen-Amundsen Basins have typically been associated with the wide continental shelves and interaction with ice shelves found in the Weddell and Ross Seas (Foldvik et al., 1985; Foster and Carmack, 1976).

The Australian-Antarctic Basin is also associated with bottom-water formation off Adelie Land (near 140°E) (Gordon and Tchernia, 1972). This bottom water is easily distinguishable from bottom waters originating from the Ross Sea as it is much fresher and colder. Previously, this source has been considered to be relatively weak, with the bottom waters found in this basin assumed to be the product of mixing Ross Sea Bottom Water (RSBW) and Weddell Sea Bottom Water (WSBW) (Carmack, 1977). However, recent hydrographic observations along 140°E have shown a local maximum in CFC-11 and oxygen concentrations and a minimum in bottom temperatures (Bindoff et al., 1997; Rintoul and Bullister, 1999). The identification of a source of bottom water on the continental shelf in the Adelie Depression near the Mertz Glacier (Gordon and Tchernia, 1972; Rintoul, 1998) has led to a reinterpretation of the volumetric census of Antarctic Bottom Waters (AABW). This reinterpretation shows that the Adelie Land Bottom Water (ADLBW) occupies 24% of the total volume of AABW around Antarctica and has the second largest volume after the Weddel Sea Bottom Water with a volume three times that of RSBW (Rintoul, 1998).

The main purpose of this hydrographic experiment is the study of the large-scale circulation and main water masses between the Antarctic Coast and the Southern Boundary of the ACC (SB) (Orsi et al., 1999). This paper investigates the water masses, the major frontal systems and the regions where there is evidence for bottom water formation. Using drifting buoy and shipboard ADCP data to provide the surface reference velocity field, the overall circulation is estimated in the zone between the Antarctic shelf break and the Southern Boundary of the ACC.

2. The measurements

The measurement program was undertaken from 30 January to 26 March 1996 as part of a multi-disciplinary experiment designed to study the large-scale ocean circulation and biology along the East Antarctic coast from 80 to 150°E. The other components of this experiment included an acoustic survey to estimate the total krill biomass, a survey of whale and bird populations, and detailed biological sampling of the mixed layer. This experiment is also complemented by a series of north–south sections undertaken by Prof T. Foster from the RV *Nathaniel B. Palmer* from 150 to 170°E (near Cape Adare) in April 1995. Together, these two experiments give

a quasi-synoptic and fairly complete coverage of the water-mass properties along the coast of East Antarctica.

Although this experiment is not formally part of World Ocean Circulation Experiment (WOCE), the oceanographic measurements are near to the WOCE accuracy standards of 0.002 pss, 0.001°C and 1% for O_2 and CFCs (Saunders, 1991). The CTD salinity has root mean square precision of 0.0027 pss and an accuracy of 0.003 pss, CTD temperature an accuracy of 0.001°C, and oxygen concentration an accuracy of 1%. For CFC-11, CFC-12 and CFC-113 accuracies of just greater than 1% were achieved. In total, 147 CTD casts were occupied, most to full depth. Underway measurements include pCO_2, SST and meteorological variables. In addition, six ARGOS drifter buoys were deployed over the continental slope between the 700 and 1500 m depths. A complete report of the physical oceanography measurement program is given in Rosenberg et al. (1997). Acoustic doppler current profiler data (ADCP) were also collected on this voyage. Limitations from the installation of the ADCP within the hull of the Aurora Australis behind an 81 mm polyethylene window, and in the accuracy of GPS and gyro heading, have resulted in certain systematic measurement biases that occur when the ship is underway. However, by using only the ADCP data collected on station, much more accurate velocities can be obtained. In this paper, we only use ADCP velocities collected when the Aurora Australis was on station or moving with a speed less than 0.35 m s^{-1}.

The experiment consisted of eight North–South CTD sections, and one irregularly spaced zonal section along approximately 63°S (Fig. 1 and Table 1). Each meridional section is approximately 200 nm long, with typically 13 CTDs in the section. To resolve the sharp features across the Antarctic Slope Front (ASF), the spacing between stations over the continental slope was often as little as 1 nm.

3. Water mass properties of surface waters

The major water masses observed in this experiment are Antarctic Surface Waters (AASW), Circumpolar Deep Water (CDW), Modified Circumpolar Deep Water (MCDW), and Antarctic Bottom Water (AABW) (Fig. 2). Throughout this paper we use neutral density variable γ (kg m^{-3}) (Jackett and McDougall, 1997). This density variable provides a simpler way of characterising the potential density of the ocean and eliminates the inconsistencies that occur in the density field, such as density inversions, through the use of a single reference pressure.

Following Whitworth et al. (1998) Antarctic Bottom Water is defined as waters with a density greater than neutral density 28.27 kg m^{-3} and warmer than -1.7°C. Antarctic Surface Waters are defined as waters lighter than neutral density 28.03 kg m^{-3}, and the water between these two densities is either Circumpolar Deep Water or Modified Circumpolar Deep Water (see also Table 2). CDW is differentiated from the MCDW by being the water with the warmest, saltiest and lowest dissolved oxygen concentration and is typically found north of the Southern Boundary of the Antarctic Circumpolar Current (ACC). Defined in this way MCDW and CDW are both circumpolar around Antarctica (Orsi et al., 1999).
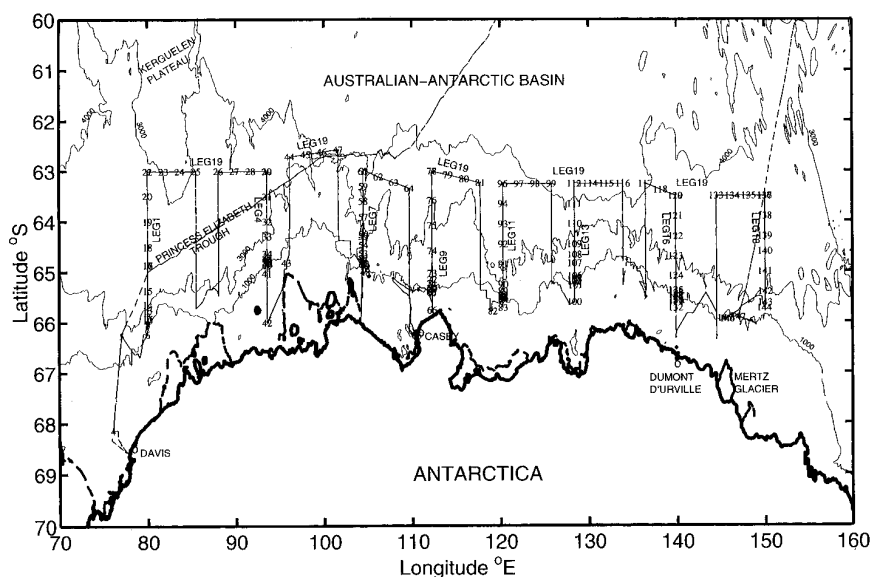
Fig. 1. The locations of major geographic features and CTD stations occupied during the BROKE experiment in January–March 1996 from the RSV *Aurora Australis*. Also shown is the cruise track (thin dashed line) and the edge of the Antarctic ice sheet (thick dashed lines). The contours are from the GEBCO bathymetric atlas.

Table 1
The nominal longitude of each meridional CTD leg, the number of stations, the most southern and northern CTD stations in the CTD leg and their corresponding station numbers (see Fig. 1)

Leg	Long. (°E)	Station no.	Start (°S)	End (°S)	Start Sta.	End Sta.
1	80	15	66.23	63.00	6	22
4	93.6	13	66.00	63.00	42	30
7	104.4	13	65.00	63.00	48	61
9	112.3	12	65.75	63.00	66	78
11	120.3	14	65.78	63.25	82	96
13	128.4	13	65.60	65.25	100	113
16	139.8	12	65.71	63.50	132	120
18	150.0	9	65.92	63.50	145	137

This definition of MCDW from Whitworth et al. (1998) is a general term for the waters found near the continental slope and includes Slope Water (Gordon and Tchernia, 1972), Prydz Bay Bottom Water and MCDW (Wong et al., 1998), all found in this sector of Antarctica, MCDW from the Ross Sea (Jacobs et al., 1970), and Modified Warm Deep Water from the Weddel Sea (Carmack, 1977). Note that AABW is denser than 28.27 kg m^{-3} and is therefore cut off by the sill across Drake Passage
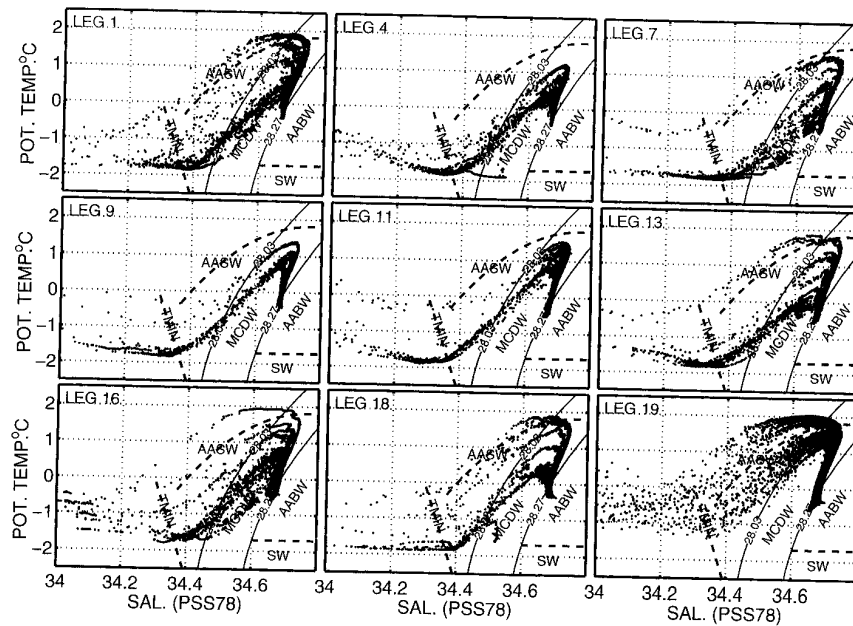
Fig. 2. Salinity (pss) and potential temperature (°C) relations for each of the north–south sections (Legs 1, 4, 7, 9, 11, 13, 16 and 18) and the composite section consisting of all the zonal legs (Leg 19). The major Antarctic water masses are shown (AASW, AABW, MCDW, SW and T Min) and are defined in the text. The two continuous lines, labelled 28.03 and 28.27, are respectively the neutral density surfaces that separate the AASW from MCDW, and MCDW from AABW. The dashed line colder than − 1.7°C separates dense (and salty) SW from AABW. The near-vertical dashed line indicates the mean location of the temperature-minimum layer. The curved dashed line is the separating line between the two classes of warm AASW discussed in the text.

Table 2

The bounding and typical properties for density, temperature and salinity variables that define each of the water masses shown in Figs. 2 and 3. Note that RSBW and ADLBW are specific types of the more general AABW

	γ (kg m^{-3})	θ (°C)	S (pss)
AASW	< 28.03	− 1.84–2.0	> 34
CDW	28.03 < γ < 28.27	> 1.8	~ 34.7
MCDW	28.03 < γ < 28.27	< 1.8	< 34.7
AABW	> 28.27	− 1.7 < θ < 0	34.65 < S < 34.72
RSBW	> 28.27	~ − 0.4	> 34.68
ADLBW	> 28.27	< 0.5	34.66 < S < 34.68
SW	> 28.27	< − 1.7	< 34.72

and consequently is not circumpolar in extent. The density surface 28.03 kg m^{-3} in this sector follows the temperature and salinity gradient that occurs at the base of the mixed layer (e.g. Fig. 4a, 5a, 6a and 7a) and is used to define the shallowest limit of

Circumpolar Deep Water. Shelf Water (SW) is the densest type of water found over the continental shelf, and is defined following Whitworth et al. (1998) to be both denser than neutral density 28.27 kg m^{-3} and colder than $-1.7°C$. Shelf water defined in this way corresponds to the high-salinity shelf water found near regions of bottom-water formation (e.g. Foster and Carmack, 1976; Jacobs et al., 1970; Rintoul, 1998). In $T-S$ space the boundaries of each of these water masses are shown in Figs. 2 and 3 and in Table 2.

The Antarctic Surface Waters (waters lighter than neutral density 28.03) (Whitworth et al., 1998) divide into three distinct classes, characterised by cold $(< -1.6°C)$, intermediate and warmer temperatures $(>0°C)$. The coldest class is only found on the meridional sections (Legs 1–18), and occurs over the shelf and continental slope. The two warmer classes of AASW are most easily seen on the $T-S$ diagram from the composite zonal section (Fig. 2, Leg 19) and lie between the MCDW and shallow temperature-minimum layer. Here the AASW falls into two distinct branches (separated by the curved dashed line in Fig. 2, Leg 19) that become progressively colder and fresher towards the temperature-minimum layer. Examination of the vertical sections (not shown) shows that the warmer type is found at the northern end of Leg 1 (early in the experiment) and further to the east on Legs 13, 16 and 18 (near the end of the experiment), and is therefore unlikely to simply be the result of the seasonal changes occurring over the duration of this experiment. The warmer type of surface water is associated with the CTD casts that also have the most saline types of CDW, while the colder type is associated with the colder and fresher MCDW. Examination of the spatial distributions of these two types of surface water on the vertical sections shows that they correspond respectively to surface waters originating north and south of the Southern Boundary of the ACC (SB) (Orsi et al., 1995).

The CDW also shows a distinct spatial structure (Fig. 2). The warmest and most saline CDW (almost 2°C) occurs at the northern end of Leg 1 in the Princess Elizabeth Trough, and then again further to the east on Legs 16 and 18 (at 140 and 150°E). On the other legs (Legs 4, 7, 9, 11 and 13) water at the salinity maximum is a significantly colder and fresher water mass by comparison, with maximum temperatures between 1.5 and 1.75°C, and is defined to be an MCDW (Table 2).

All of the meridional legs (except 18) crossed the shelf break, but most did not penetrate the ice cover far enough to sample fully the deep depressions found near the Antarctic Coastline. The only deep depression actually sampled in this survey was at station 42 near the Shackleton Ice Shelf (Leg 2) at 94°E. This depression is deeper than 1228 m and has no direct means of communicating with the open ocean. This depression should therefore contain relic winter water. The $T-S$ properties of this cast can be seen in Fig. 2, Leg 4 as the near-freezing salty profile in MCDW density range. However, the water in this depression is not dense enough (that is < 28.27 kg m^{-3}) and is too fresh (34.532 pss) to be classed as SW, which suggests that bottom waters are unlikely to form near the Shackleton Ice Shelf.

The AABW properties vary significantly between Legs 1 and 18 and can be grouped into two classes (Figs. 2 and 3). On Leg 18 (150°E) the $T-S$ relation (Fig. 3, Leg 18) shows the presence of a saline, relatively warm water mass (which is also lower in oxygen and CFC-11) that has its origin in the Ross Sea (Gordon and Tchernia, 1972).
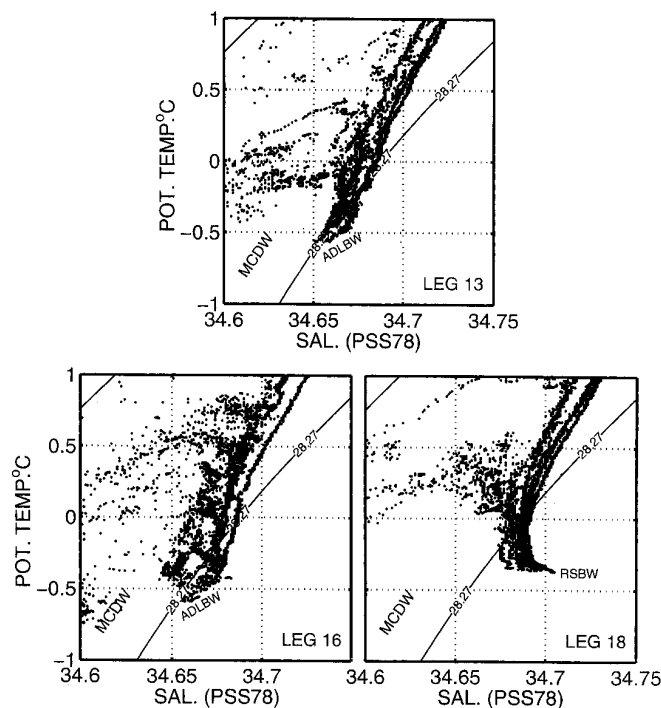
Fig. 3. Salinity (pss) and potential temperature (°C) relations for Legs 13, 16 and 18 detailing the RSBW and ADLBW bottom waters found in this region. The two continuous lines, labelled 28.03 and 28.27, are respectively the neutral density surfaces that separate the AASW from MCDW, and MCDW from AABW.

This pronounced signal of the Ross Sea Bottom Water (RSBW) in Leg 18 is much weaker in Leg 16 (140°E) just 10° of longitude away (Fig. 3, Leg 16), and further west at Leg 13 there is no significant evidence for a contribution from RSBW. On CTD Legs 13 and 16 the westward flowing RSBW has been replaced by Adelie Land Bottom Water (ADLBW). ADLBW is much colder and fresher (− 0.55°C, 34.66 pss) compared to RSBW (− 0.35°C, 34.71 pss) (see Fig. 3), and it is this water mass that dominates the T–S properties below 28.27 density surface in the Australian-Antarctic Basin. It can be seen from the water-mass properties that the ADLBW must originate between 150 and 140°E (Legs 18 and 16).

4. Frontal features

All of the north–south CTD sections (except Leg 18) cross the shelf break onto the continental shelf. With a typical length of 200 nm, most of the sections only extend to, or are just south of the SB in this region. The exceptions are Legs 1, 13 and 18, which

cross the SB. The first north–south section (Leg 1) is just west of the shallowest point of the Princess Elizabeth Trough (Fig. 1) and the bottom waters here are part of the bottom waters associated with the Weddell-Enderby Basin (Rodman and Gordon, 1982; Speer and Forbes, 1994). All of the other meridional sections fall within the Australian-Antarctic Basin.

Here we show four of the seven sections (Legs 7, 9, 11 and 16) from the Australian-Antarctic Basin to demonstrate the variations in the structure of the Antarctic Slope Front and the distribution of the major water masses over/near the continental shelf break. Perhaps the most typical CTD section in this region is from Leg 9 at 112°E (Fig. 4a and b). We define the Antarctic Slope Front (ASF) as the strong sub-surface horizontal temperature and salinity gradient that separates the light Antarctic Surface Waters (AASW) from the denser Modified Circumpolar Deep Water (MCDW) (see also Whitworth et al., 1998). This maximum sub-surface gradient generally, but not always, lies north of the shelf break in water in depth range of approximately 200–500 dbar. In the case of Leg 9 (Fig. 4a and b) the Antarctic Slope Front shows a very pronounced horizontal temperature, salinity and density gradient between the 3rd and 4th stations from the southern end. The position of the 28.03 density surface, which separates the AASW from the MCDW, also deepens rapidly in the ASF, and on this section the ASF is characterised by a strong horizontal density gradient. Note also that this density surface follows the depth of the winter mixed layer in the open ocean, justifying this choice of density for separating AASW from MCDW. In this section the Antarctic Surface Waters occupy the entire volume of the shelf, and the section has a temperature–salinity structure similar to the sections found in the eastern Weddell Sea (15°E) (Heywood et al., 1998), eastern Prydz Bay (81°E) and the eastern Ross Sea (Whitworth et al., 1998).

Although there is a thick wedge of AABW in this section, i.e. water deeper than the 28.27 kg m^{-3} density surface, this density surface intersects the continental slope at a large angle and thus there is no direct evidence for the active formation of AABW with dense waters cascading down the continental slope (see also Baines and Condie, 1998). Over the continental slope only MCDW is found (that is density between 28.03 and 28.27 kg m^{-3}).

One of the interesting features of this section is the two cold-core eddies or meanders observed in temperature, salinity, oxygen and silicate data offshore from the ASF (Fig. 4a–d). Because of the sparse longitudinal spacing between the sections, the east–west extent of these features is unresolved and it is unknown whether they are isolated eddies or simply meanders of the Antarctic Slope Front (or alternatively meanders from the SB). We refer to these cold-core eddies or meanders as "features" for convenience. The first cold feature occurs over the continental slope (seven stations north of the southern end) in 1800 m deep water, and the second over the bathymetric high (64.5°S, nine stations from the southern end). Below 500 dbar these cold features are associated with decreased salinity, and increased oxygen and silicate concentrations (Fig. 4a–d). Cyclonic eddies have been noted in this sector (Wakatsuchi et al., 1994), some of which appear to be permanent. The cold feature found on this leg (at 112°E) is on the western side of a semi-permanent cyclonic eddy found at 115°E (Wakatsuchi et al., 1994).
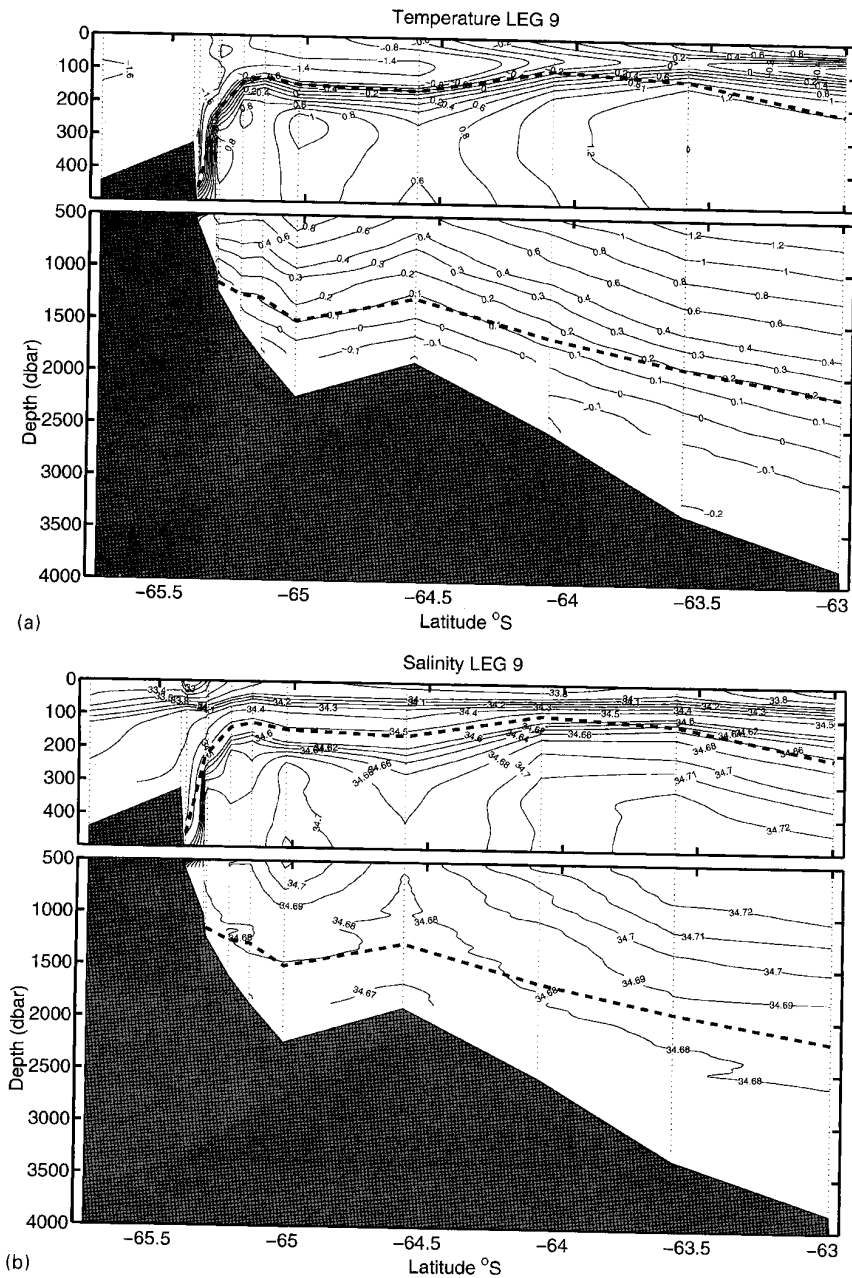
(a)

(b)

Fig. 4. Vertical sections of (a) temperature (°C), (b) salinity pss, (c) oxygen (μm l⁻¹) and (d) silicate (μm l⁻¹) along Leg 9. Leg 9 is located at 112°E. The thick dashed lines are respectively the depths of the neutral density surfaces 28.03 and 28.27 kg m⁻³. The fine dotted lines are the location of each cast and the crosses in (c) and (d) are depths of water samples. Note the expanded scale in the upper panel.
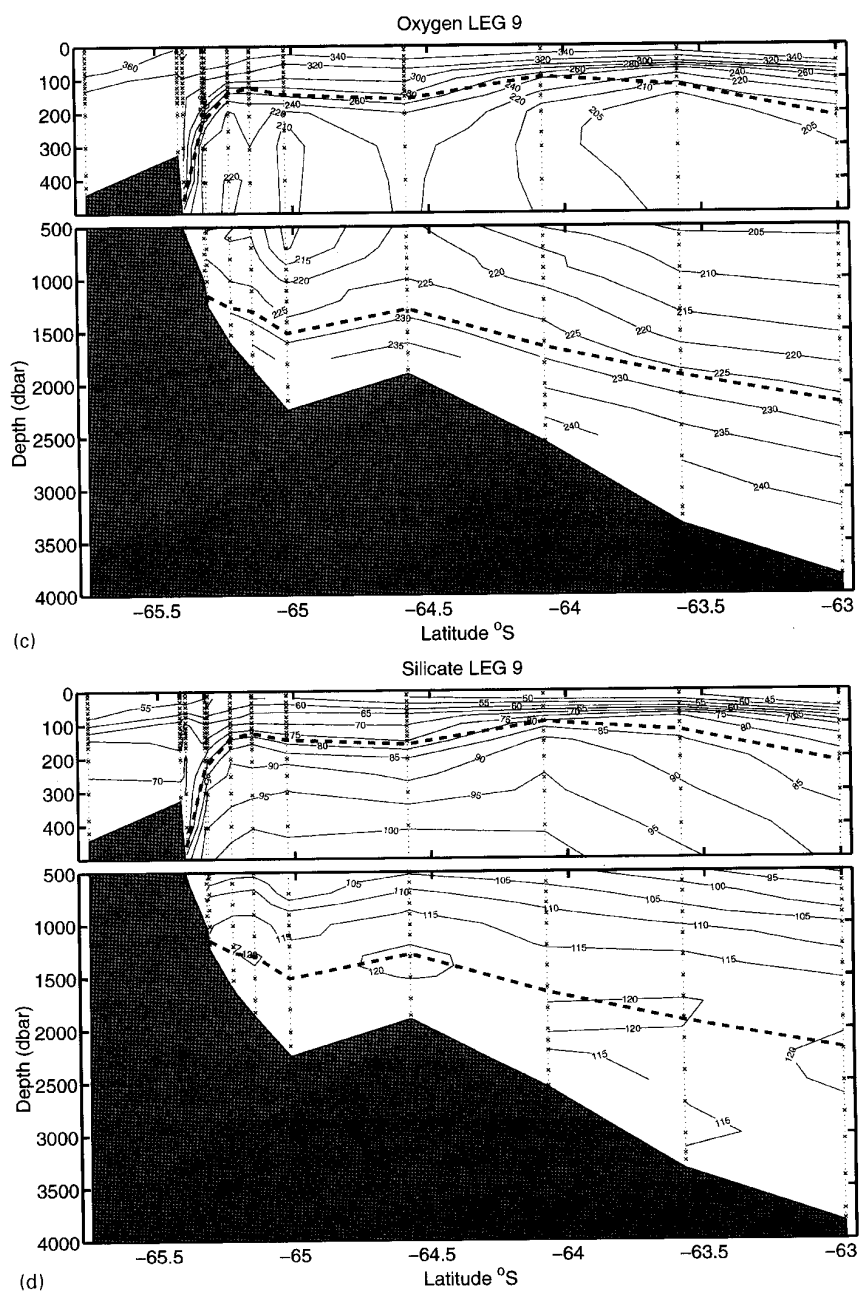
Oxygen LEG 9

(c)

Silicate LEG 9

(d)

Fig. 4 (*continued*)

Leg 11 at 120°E is 8° east of Leg 9, and shows quite different water-mass distributions over the shelf and continental slope. The shape of the continental slope is steeper on this section and offshore has a more regular bottom topography. The ASF, as defined by a strong horizontal temperature, salinity, and density gradient, occurs inshore of the continental shelf break between stations 2 and 3 on this section (Fig. 5a and b). However, these horizontal gradients are weaker and the waters on the shelf break are warmer, saltier, denser, poorer in oxygen and richer in silicate than for the corresponding position on Leg 9. The water over the shelf break here is MCDW (i.e. has neutral density between 28.03 and 28.27 kg m^{-3}), and this is the only section in this survey where the presence of MCDW over the continental shelf is observed. A warmer type of MCDW, represented by the 1.2°C isotherm, is just 4.7 nm from the shelf break and this isotherm is closer to the shelf break here than on any of the other sections.

On this section the AASW (neutral density < 28.03 kg m^{-3}) forms a wedge of water, thickest over the shelf and smoothly thinning towards the SB. Although the ASF is weak in the upper 500 dbar of the water column there is a significant increase in the depth of isotherms, isohalines and density surfaces over the continental slope (between the 3rd and 6th stations, Fig. 5a and b), suggesting a westward flow with respect to the bottom (or eastwards with respect to the surface) with a strong eastward flow relative to the bottom immediately to the north.

The silicate concentrations show a well-defined pattern in the MCDW (at ~ 1000 dbar) on this section (Fig. 4d). In the region with eastward shear, the silicate values are high, decrease, and then increase again in the northern part of the section. The silicate values immediately over the continental slope in the region of westward shear are much lower. This pattern occurs over the entire depth range of MCDW. The AABW south of 64°S shows low silicates compared with the northern most station on this section. The lowest silicate concentrations occur nearer to the continental slope and are the result of low silicate values associated with the formation of bottom water further east (discussed below). On Leg 9 the silicate values in the AABW are higher than on Leg 11 (respectively > 115 μm l^{-1} and < 105 μm l^{-1}) suggesting that the bottom waters have moved offshore where the ocean depth is deeper. The pattern of silicates in MCDW on Leg 9 (Fig. 4d) has some similarities to the pattern in Leg 11, except that here the cold features make the identification of the silicate adjacent to the coast and offshore less certain.

The last two sections (Legs 9 and 11) are examples of where there is no direct evidence of water-mass formation occurring. In contrast, the CTD sections along Leg 7 at 104°E and Leg 16 at 140°E show very distinctive and different patterns of water formation over the continental slope (Figs. 5 and 6).

On Leg 7 the ASF occurs offshore, between stations 3 and 4 from the shelf break where the gradients of temperature and salinity are strongest, and the 28.03 kg m^{-3} neutral density surface is deepest. ASF on this section shows a "V" shaped structure where the AASW water (< 28.03 kg m^{-3}) is thick at the ASF and then shoals towards the shelf break. Due to the presence of sea ice, no stations were occupied further inshore of the shelf break to determine if denser and more saline waters occurred on the shelf floor. On the continental slope from the shelf break to 1500 dbar there is
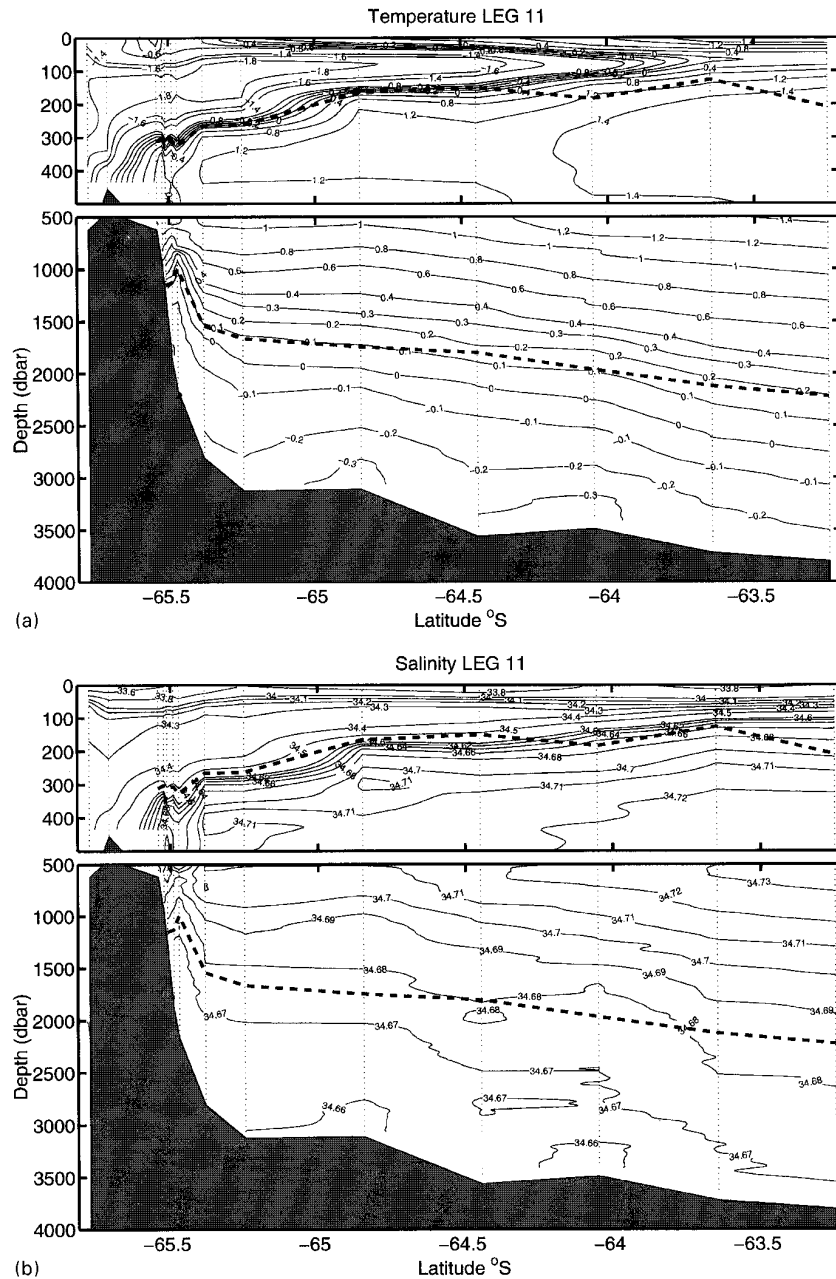
(a)

(b)

Fig. 5. Vertical sections of (a) temperature (°C), (b) salinity (pss), (c) oxygen (μm l^{-1}) and (d) silicate (μm l^{-1}) along Leg 11. Leg 11 is located at 120°E. The thick dashed lines are respectively the depths of the neutral density surfaces 28.03 and 28.27 kg m^{-3}. The fine dotted lines are the location of each cast and the crosses in (c) and (d) are depths of water samples. Note the expanded scale in the upper panel.
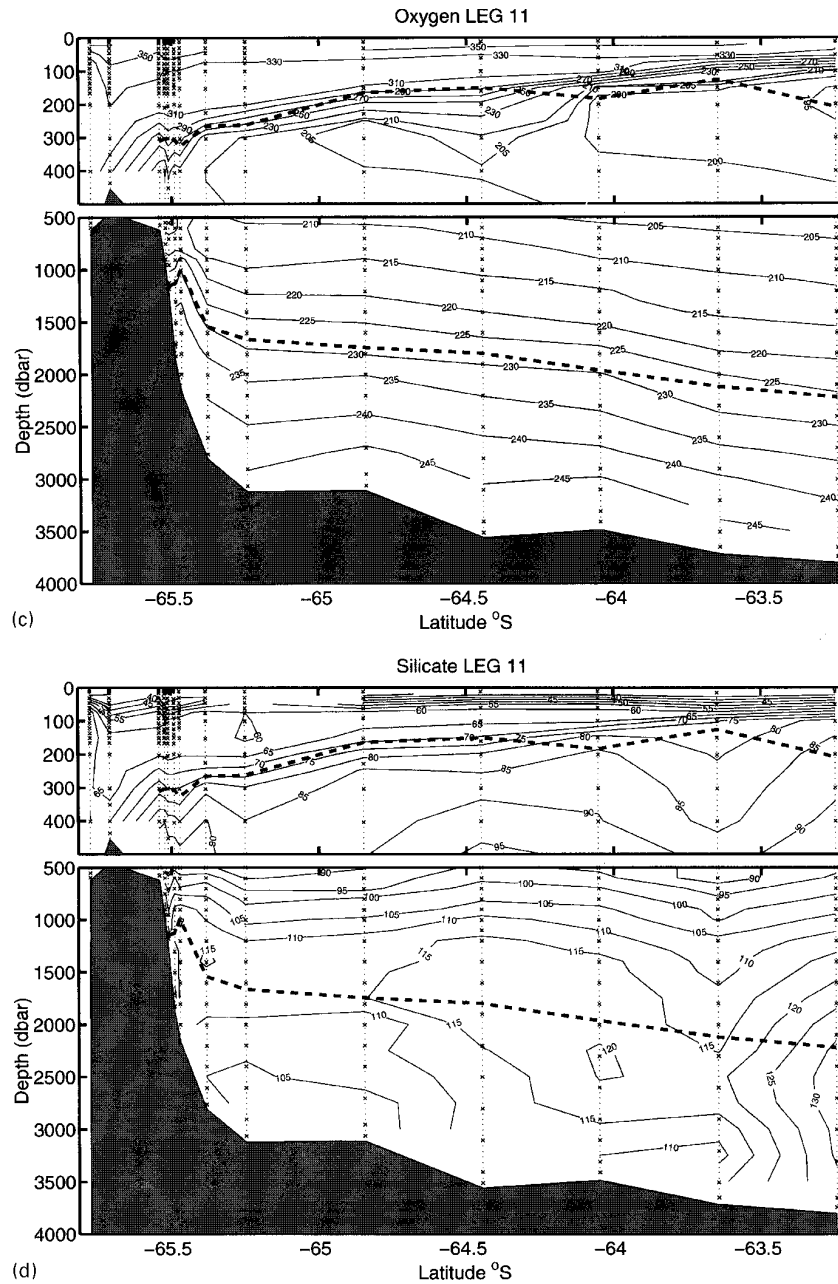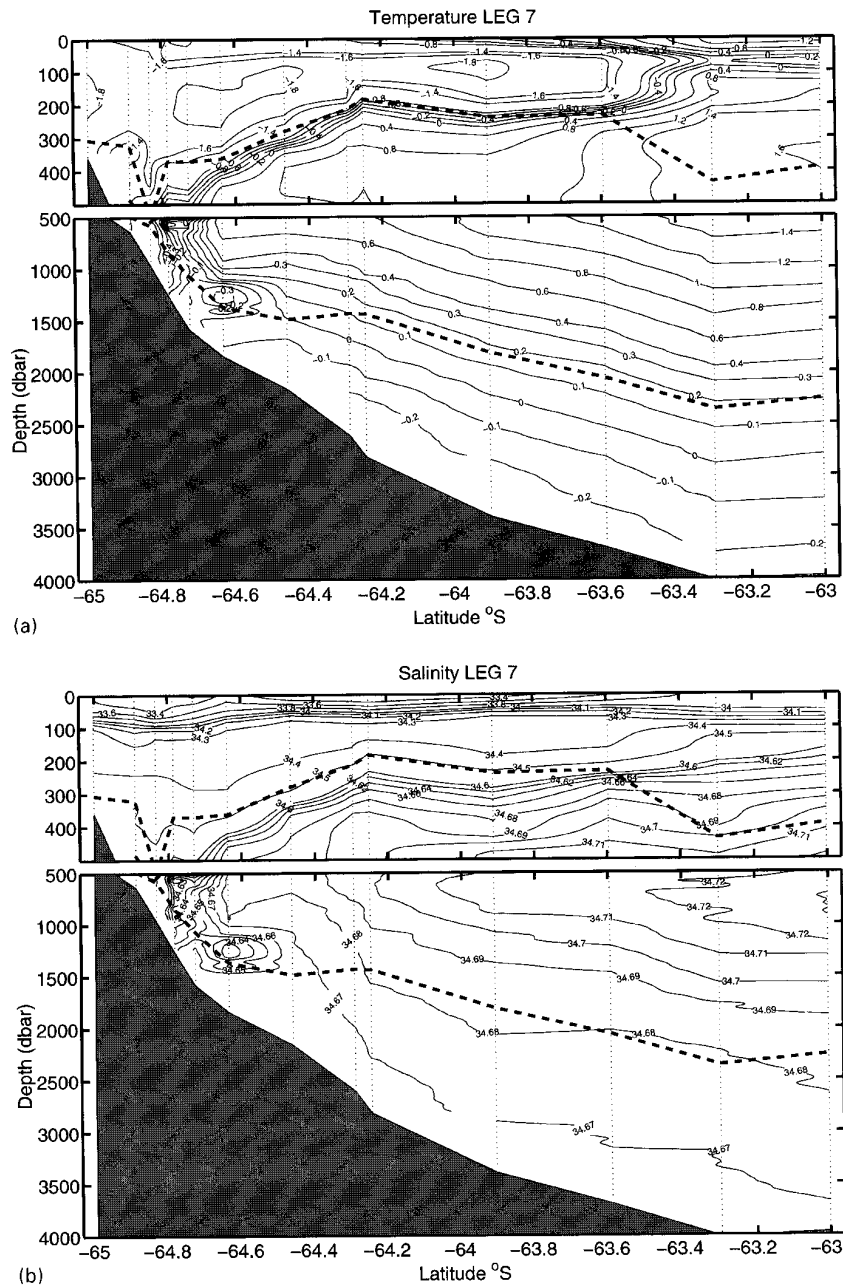
Oxygen LEG 11

(c)

Silicate LEG 11

(d)

Fig. 5 (continued)

Temperature LEG 7

(a)

Salinity LEG 7

(b)

Fig. 6. Vertical sections of (a) temperature (°C), (b) salinity pss, (c) oxygen (μm l^{-1}) and (d) silicate (μm l^{-1}) along Leg 7. Leg 7 is located at 104°E. The thick dashed lines are respectively the depths of the neutral density surfaces 28.03 and 28.27 kg m^{-3}. The fine dotted lines are the location of each cast and the crosses in (c) and (d) are depths of water samples. Note the expanded scale in the upper panel.
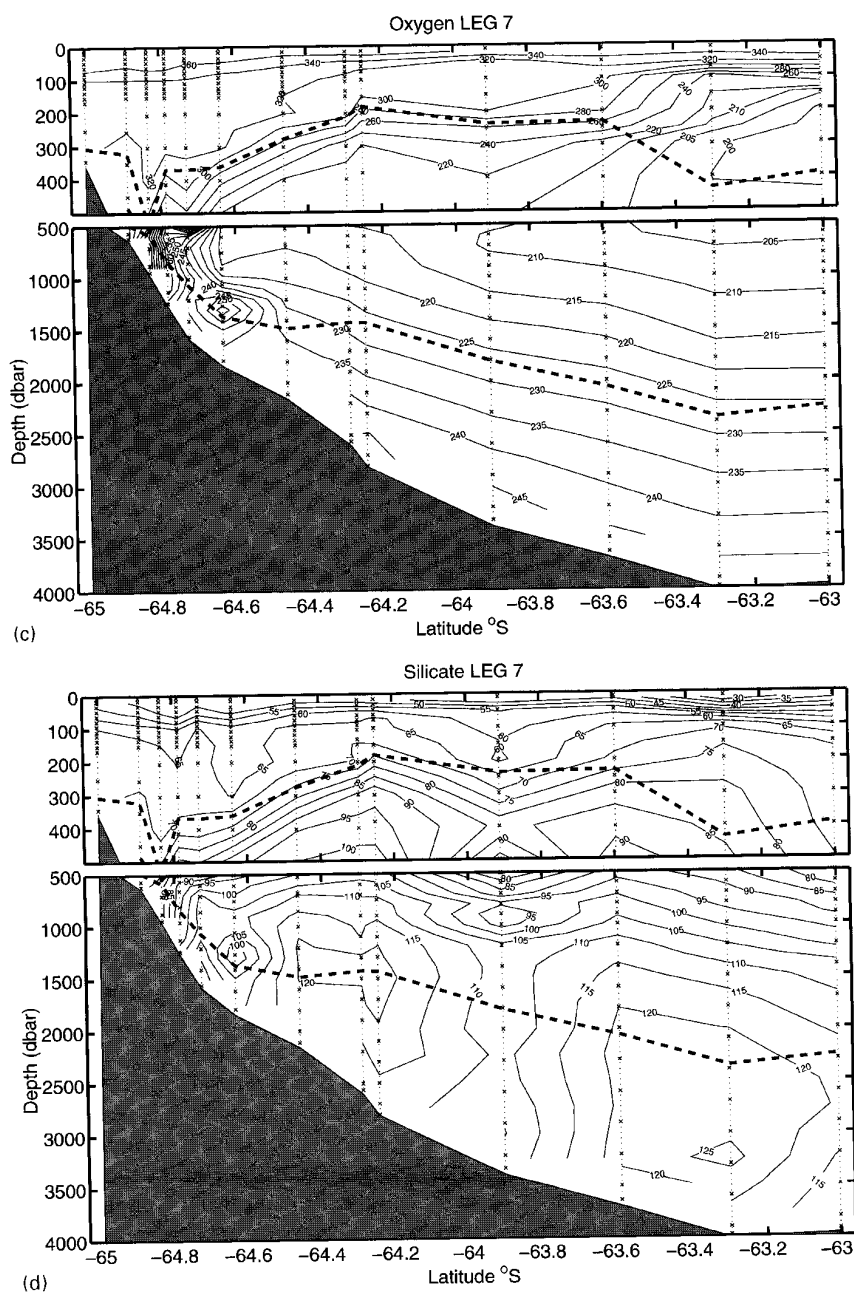
(c)

(d)

Fig. 6 (*continued*)

a distinctive layer of cold, fresher, oxygen-rich, silicate-poor water (Fig. 6a–d) with a high CFC-11 concentration (not shown). Just offshore from this cold layer there is a single discrete parcel of water that has very distinctive water-mass properties, and also with similar characteristics to the cold layer on the slope just to the south. A total of five CTD stations sample these waters on the continental slope. The water masses in the discrete parcel and plume over the slope are almost identical and probably come from the same source. Note that this layer is colder and fresher than the AABW below that originates further to the east.

Although there is a continuous layer of this anomalous water down the continental slope on Leg 7, it is not dense enough to sink all the way down the continental rise. The neutral density surface 28.27 kg m^{-3} intersects this layer as it spread outs into the ocean interior and in this case only results in the formation of MCDW rather than the formation of true AABW.

The sections to the east and west (i.e. Legs 4 and 9) both have strong ASF fronts (e.g. Fig. 5a) and neither show any evidence of active MCDW formation. It seems probable that this plume has originated nearby from the shelf region between 104.4 and 112.3°E (Legs 7 and 9), west of Casey (Fig. 1). The pattern of silicates (Fig. 5d) in this section on the density surface 28.27 kg m^{-3} shows a similar pattern to the silicates on Leg 11, with a local maximum offshore of 120 μm l^{-1} that decreases to the north and then increases again near 63.5°S.

Like the previous section, Leg 16 at 140°E shows active water formation in this region, and in this case extends fairly continuously down to the bottom (Fig. 7). The ASF is located on this section between the 2nd and 3rd cast from the shelf break. Although there are strong gradients in temperature and salinity, the gradient in the slope of the 28.03 kg m^{-3} neutral surface is relatively weak (cf. Leg 9), suggesting a relatively weak westward surface current. The structure of the AASW is complex here, as represented by the 28.03 kg m^{-3} density surface, with the layer deeper over the shelf break, thinning in the ASF to a local minimum between the 6th and 7th stations and then deepening to approximately 300 dbar at $\sim 65°$S before shallowing again. This thickened AASW at 65°S coincides with a deepening of the isotherms and isohalines, reduction in silicates, and increased oxygen in the upper 1000 dbar. This cold-core feature in the upper 1000 dbar is qualitatively similar to the shallow cyclonic feature observed in Leg 9 (Fig. 4a and b) and is similar to those features reported by Wakatsuchi et al. (1994), although in this case farther east. Leg 18 (not shown here) also has a qualitatively similar pattern in the temperature and salinity fields.

Over the continental slope the $-0.2°$C isotherm is continuous from the shelf break down the slope and onto the rise at 65°S. Close examination reveals that the actual sea-floor temperatures over the slope are slightly warmer than those observed over the continental rise (Bindoff et al., 1997), suggesting that the coldest type of bottom water observed in deeper water on the rise is either formed during winter or channelled down canyons over the continental slope. Temperature measurements from moorings in water depth of 2632 m on this section show that the coldest temperatures occur between July and December (Fukamachi et al., 2000). Nevertheless, the strong upward slope of the 28.27 density surface right to the shelf break in this section shows that AABW water mass is continuous to the shelf break here. The source of bottom
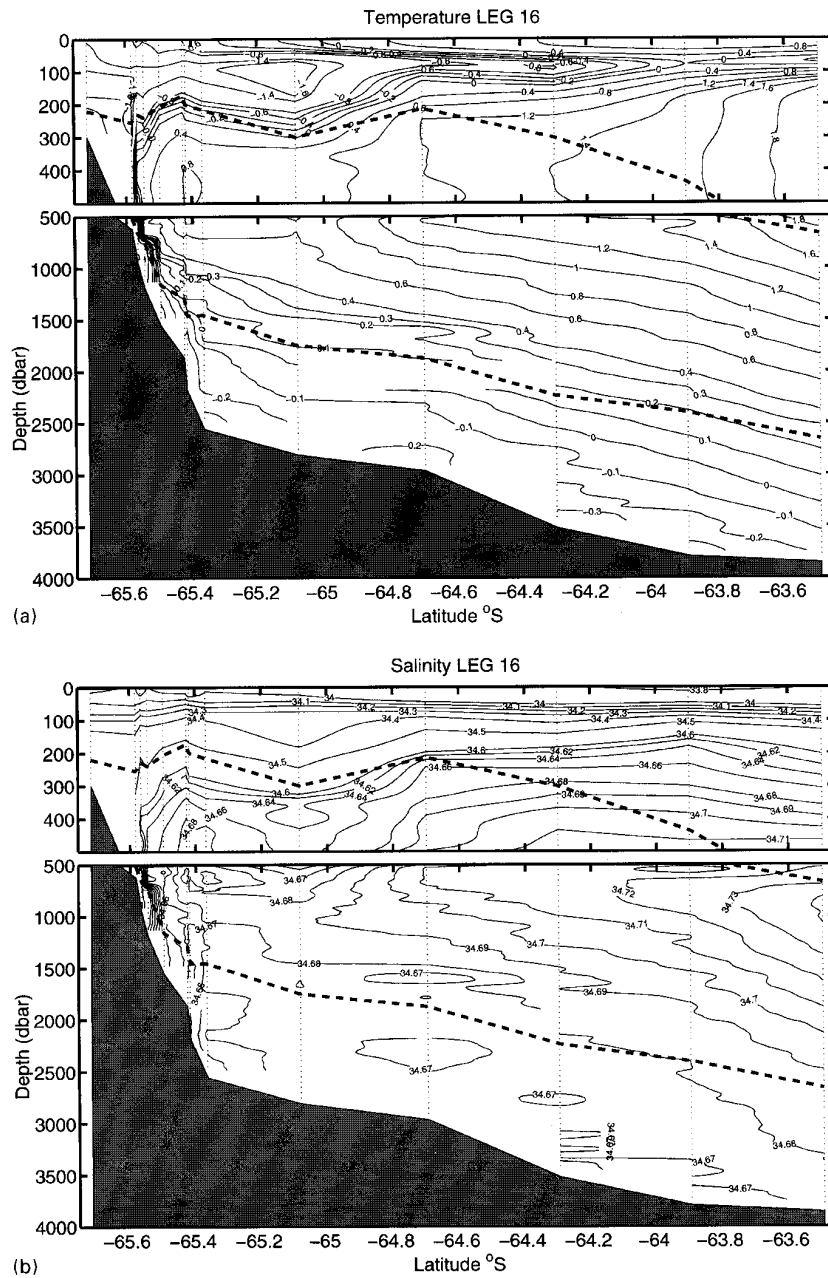
Fig. 7. Vertical sections of (a) temperature (°C), (b) salinity (pss), (c) oxygen (μm l^{-1}) and (d) silicate (μm l^{-1}) along Leg 16. Leg 16 is located at 140°E. The thick dashed lines are respectively the depths of the neutral density surfaces 28.03 and 28.27 kg m^{-3}. The fine dotted lines are the location of each cast and the crosses in (c) and (d) are depths of water samples. Note the expanded scale in the upper panel.
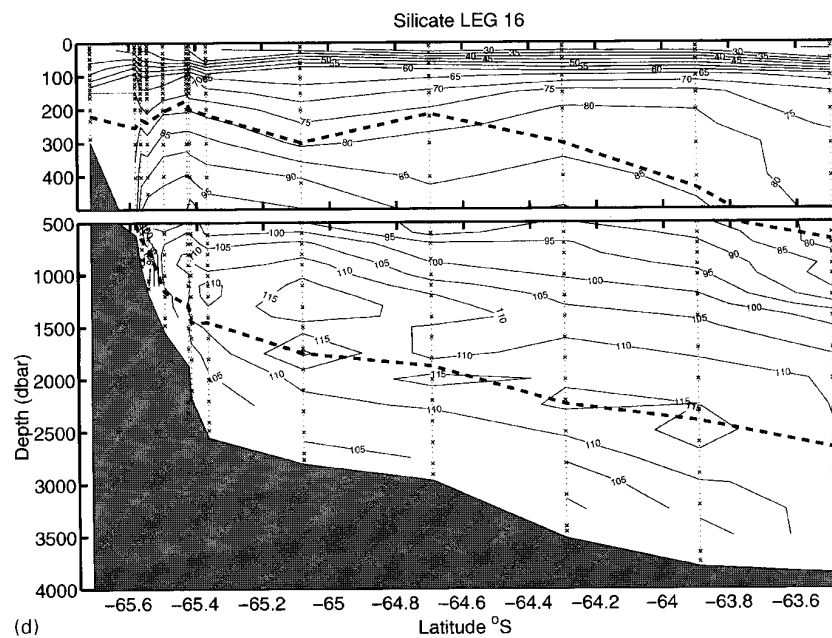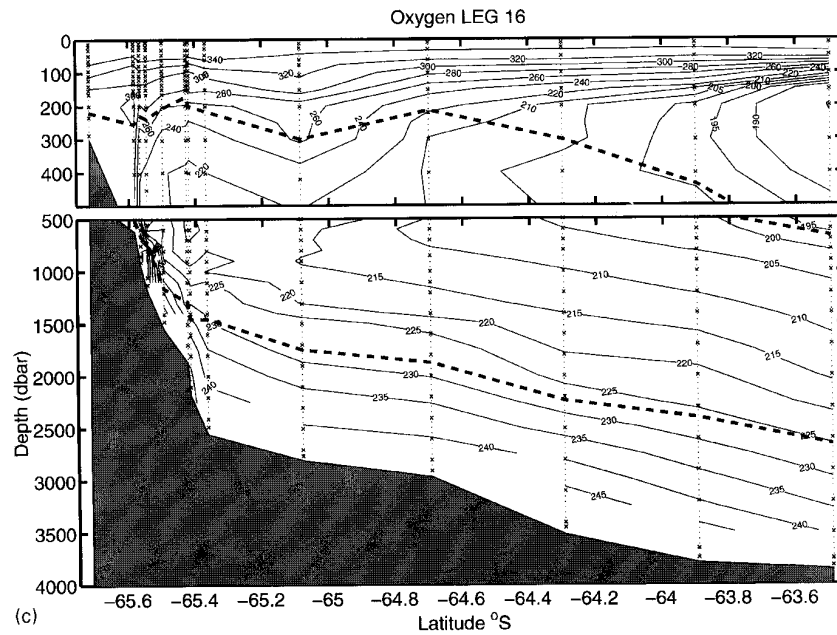
Fig. 7 (*continued*)

water is likely to be the Adelie Depression at about 142–146°E (Gordon and Tchernia, 1972; Rintoul, 1998). If the 28.27 kg m^{-3} density surface is taken as a reference level, then the density field over the continental slope suggests that the current on the sea floor is westward and bottom-intensified, consistent with the bottom-water-mass properties described in the previous section (see also the next section).

5. Large-Scale circulation and horizontal distributions of properties

Special problems arise in determining the circulation between the Antarctic continent and the SB. The velocity shear from the density field and pattern of tracers give relatively few direct clues. From surface meteorology the Antarctic Divergence is defined as the point where the average winds change from eastwards (westerlies) to westwards (easterlies). The wind-stress curl is a maximum there and causes the Antarctic Divergence to be a point of strong upwelling. The oceanographic expression of this upwelling is often interpreted as the point where the temperature minimum is shallowest (Fig. 8). North of the ASF, the temperature minimum layer is 60–100 m deep, with relatively weak meridional gradients in the depth of this layer. Typically the eight CTD sections do not extend north of the Antarctic Divergence, and there is strong natural variability between CTD casts. As a consequence of these factors, the

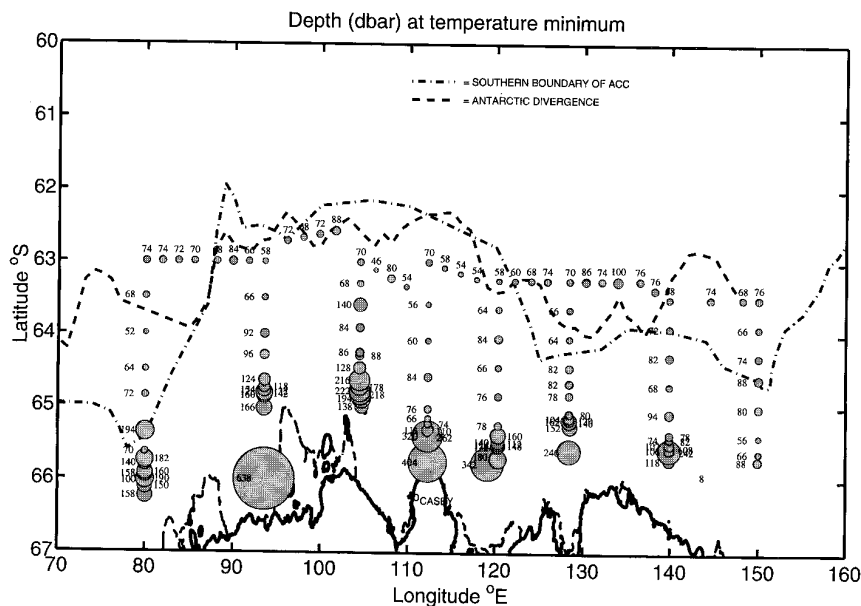Fig. 8. Depth of the temperature minimum (dbar). The size of the circles indicates the depth of temperature-minimum layer with actual depths given by numbers above or to the left. The thick dashed line is the location of the Antarctic Divergence inferred from surface drifter data (Heil and Allison, 1999) and the thick dot–dashed line is the location of the Southern Boundary of the ACC (Orsi et al., 1995).

precise position of the Antarctic Divergence is not easily determined from these data alone. However, comparisons of the depth of the temperature-minimum layer with the position of the Antarctic Divergence inferred from 39 drifting buoys deployed between 1985 and 1996 (Heil and Allison, 1999) do show a good correspondence (Fig. 8). This comparison is best in the Princess Elizabeth Trough (Legs 1 and 4), and in the eastern part of the survey on Legs 13, 16 and 18. On these legs the temperature-minimum layer is shallowest and corresponds almost exactly with the position of the Antarctic Divergence as identified from the drifting buoy data. On the meridional Legs 7, 9 and 11, the position of the Antarctic Divergence is slightly to the north of these sections as determined from the buoy data (Fig. 8).

Another oceanographic feature that is relevant to this survey is the Southern Boundary of the ACC (SB) (Orsi et al., 1995) (Fig. 8), which has been identified as being an important boundary in biological production (Tynan, 1998). The SB is interpreted here as the southernmost boundary of the eastward flowing ACC and is defined by the southernmost extent of the oxygen minimum where the temperatures are $> 1.5°C$ and salinities > 34.5 pss (Orsi et al., 1995). Identification of the SB in the BROKE data agrees with the location of the SB defined by Orsi et al. (1995) and shown in Fig. 8. In the Princess Elizabeth Trough (at 85°E) and east of 140°E the Antarctic Divergence and SB diverge, with the SB appearing to be further south than the divergence as identified from surface velocity field obtained from the buoy drift data. In the region from 85 to 135°E the position of the divergence and the SB are coincident and represent the same oceanographic features over approximately 71% of the experiment area.

The mean winds south of the divergence are westward, causing an Ekman transport towards the Antarctic Coast. Simple theory predicts that this Ekman transport against the coast would support a westward geostrophic circulation below the wind-driven mixed layer. In addition, in this region the density stratification is quite weak and the vertical shear of the density field is positive north of the ASF (Figs. 4–7), making the appropriate choice of reference level uncertain for estimating ocean transports. This uncertainty in reference level is also particularly important over the continental shelf and slope regions. Six buoys, similar to the WOCE surface velocity programme drifters, were deployed as part of the experiment to help resolve this choice of reference level. All of the buoys were deployed with a 6 m "holy sock" type drogue over the continental slope in water depths of between 1000 and 1500 m (Fig. 9).

The most striking result from the buoy tracks is their correlation with bottom topography, particularly over the continental slope 100°E. This correlation with the bottom topography tends to have shorter scales than the large-scale winds, and suggests that much of the buoys' path is determined by the ocean currents. All of the six buoys deployed as part of this experiment move westwards along the continental slope. Buoy speeds over the continental slope are strongly westwards averaging 0.16 m s^{-1} for water less than 500 m and decreasing to zero in water depth of 3800 m. For greater ocean depth, the speed becomes eastward.

The spatial coverage of the survey region by the buoys is relatively incomplete, particularly in the region of the SB or Antarctic Divergence. However, shipboard ADCP estimates of the surface velocity at the CTD stations provide a better spatial
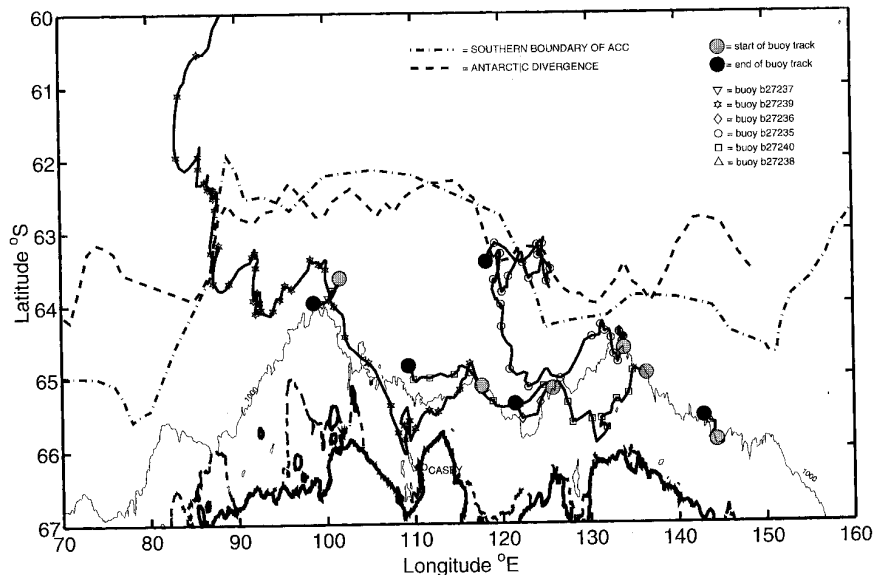
Fig. 9. The drifter tracks of the six buoys deployed during the BROKE experiment. The thick dashed line is the location of the Antarctic Divergence inferred from surface drifter data (Heil and Allison, 1999) and the thick dot–dashed line is the location of the Southern Boundary of the ACC (Orsi et al., 1995). Each buoy is differentiated by a different symbol shown in the legend.

coverage than the drifting buoys (cf. Fig. 1 with Fig. 9). We, therefore, use the ship-based ADCP data as the reference velocity field for the CTD data because of the superior spatial coverage.

The velocity data from the ADCP at all of the CTD stations were interpolated using optimal mapping. A Gaussian correlation function was assumed with a length scale of 100 km. The root mean square (rms) error between the mapped data and the direct observations is 0.06 m s^{-1} and the typical posteriori errors after interpolation are between 0.06 and 0.1 m s^{-1} at each grid point. These errors are smaller than the observed speeds along the shelf break, and north of the SB (Fig. 10a), suggesting that much of the large-scale velocity field is statistically significant. The smoothed velocity field at 28.6 m depth level (Fig. 10a) shows a pattern consistent with the buoy drift tracks. Each meridional section (except Leg 1) shows a strong westward flow along the Antarctic continental shelf and slope, largely parallel to bottom topography like the buoys drift tracks shown in Fig. 9. On Leg 1, the weak eastward flow over the continental slope could be part of the clockwise gyre off Prydz Bay. On each leg this westward flow changes to an eastward flow offshore. On Legs 4, 7, 9 and 16 the point where the flow changes sign is well south of the location of the SB and Antarctic Divergence. On Legs 1, 13 and 18 the point where the flow changes sign agrees well with the location of the SB but not with the Antarctic Divergence. Although the instrument and oceanographic noise in the ADCP data is quite large compared to the

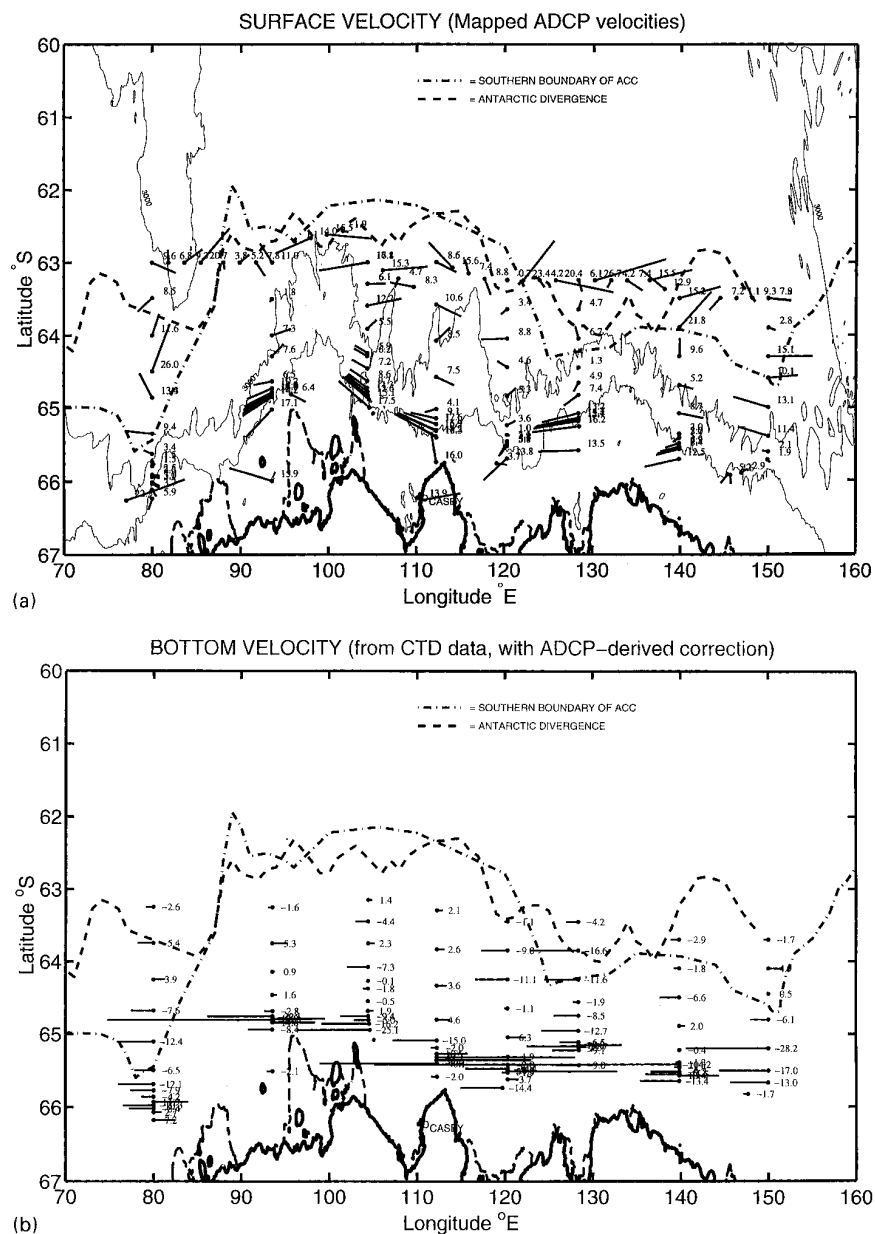Fig. 10. (a) The surface velocity from the ADCP data at 28.6 m depth for each of the CTD stations shown in Fig. 1, and (b) the adjusted eastward CTD bottom velocity using the eastward component of the ADCP data at 28.6 m as the reference velocity field. The ADCP data were objectively mapped to the mid-point positions between the CTD casts. The numbers to the right of the "arrows" are the speed of each vector in cm s^{-1}.

observed surface velocities, the eastward flow south of the SB between 90 and 115°E suggests a recirculation of the westward current over the continental shelf, perhaps forming part of a gyre nested between the Antarctic continent and the Southern Boundary of the ACC.

The ADCP velocity data (and drifting buoy data), and the distribution of the bottom water masses provide constraints for determining the approximate reference level for the CTD data. The distributions of CFC-11, oxygen and potential temperature over the continental rise suggest a westward flow on the sea floor (Bindoff et al., 1997), and the surface velocity data also imply a westward surface flow over the shelf, slope and rise regions. Using the eastward component of the surface velocity data as a reference velocity the bottom-velocity pattern can be calculated, using the velocity shear from the thermal wind equations at the midpoint of each station pair (Fig. 10b). Because the vertical velocity shear is positive upwards where the surface ADCP flow is eastward (Fig. 10a), the magnitudes of the bottom velocities are smaller than the surface velocities, and tend to be westward on average.

In the slope region, where the surface flow is westwards, the vertical shear is more complex, but typically is positive upwards leading to bottom intensification of the flow. The vertical shear between the surface and bottom has a maximum $0.17 \, \text{m s}^{-1}$ and is commonly greater than $0.1 \, \text{m s}^{-1}$. This intensification is particularly strong on Legs 13, 16 and to a lesser extent on Leg 7 (see Figs. 6a and 7a and the difference between Figs. 10a and b).

Recent current meter results from along Leg 16 (at 139°59′E, 65°10′S) in 2632 m deep water show a strong intensification of the current speed through the water column. The mean bottom speed for this mooring for the 13-month period is approximately $0.16 \pm 0.05 \, \text{m s}^{-1}$ compared to $0.05 \pm 0.04 \, \text{m s}^{-1}$ at 1075 m (Fukamachi et al., 2000). For a similar depth on this leg the estimated bottom velocity is between 0.09 and $0.11 \, \text{m s}^{-1}$ (Fig. 10b), which compares reasonably well with the current meter observations. Surface velocities and bottom velocities derived from the combined use of CTD and ADCP data (using a more accurate vector GPS system) in the Princess Elizabeth Trough showed strong westward flows at the sea floor south of SB in excess of $0.05 \, \text{m s}^{-1}$ (Heywood et al., 1999).

6. Discussion and conclusions

The distributions of water masses of each of the meridional sections suggest that the continental shelf, break and slope regions have complex water-mass and frontal structures that vary along the entire survey area (Table 3). On most of the sections there is evidence of gradients in the ocean interior that suggest the presence of cyclonic eddies or meanders. Some of these features in the vertical sections coincide with the cold cyclonic eddies identified by Wakatsuchi et al. (1994), but extend their results along the entire domain of the survey.

The slope front also varies its location relative to the shelf break and its strength in the meridional sections. The observation of MCDW over the continental shelf on Leg 11 has important implications for the salinity of the shelf waters and for the

Table 3

Summary of hydrographic features on each section. In column 2, the ASF is either one sided (1) or V shaped, and weak or strong; column 3 is the position of the ASF with respect to the shelf break; column 4 is the way the 28.27 kg m^{-3} density surface intersects the continental slope; and columns 5 and 6 indicate the presence of a salinity maximum on the 28.27 kg m^{-3} density surface over the continental rise and slope

Leg	ASF shape	ASF position	AABW	Max, rise	Max, slope
1	1, strong	North	Cut off	Yes	Yes
4	1, strong	North	Cut off	?	Yes
7	V, weak	North	Shelf br.	Yes	Yes
9	1, strong	North	Cut off	Yes	Yes
11	1, weak	South	Cut off	Yes	Yes
13	1, weak	North	Raised	Yes	No
16	1, strong	North	Shelf br.	Yes	No
18	?	North	?	Yes	?

exchange of heat from offshore onto the shelf. Although such tongues of MCDW over the shelf have been inferred from observation, evidence for the direct invasion of MCDW onto the shelf is relatively rare in this region of Antarctica. This is in contrast to the West Antarctic Peninsular where flooding of the continental shelf by MCDW is common (Hoffman and Klinck, 1998). The transport of more salty MCDW on the shelf has an important role in the formation of bottom waters (Wong et al., 1998), and also in the supply of oceanic waters to the shelf region. However, the MCDW observed on Leg 11 over the shelf is relatively cold and fresh ($-1.4°$C and 34.45 pss) compared to the MCDW found in the Adelie Depression ($> -0.5°$C) (Rintoul, 1998), suggesting that the area of Leg 11 is unlikely to be a source of bottom waters.

The shape of the slope front is also important. On Leg 7 the AASW has a conspicuous "V" shape in its thickness over the continental slope. This is also the section that shows the presence of a plume of dense water flowing down slope and forming water in the MCDW density range. This V shape in the thickness of AASW across the ASF is similar to that observed in the western Weddell Sea (Gill, 1973; Whitworth et al., 1998), a recognised bottom-water-formation region, and has been linked to theories for bottom-water formation (Gill, 1973). In addition, such plumes that spread into the ocean interior at mid-depth are important for ventilating this density range and represent one way in which the MCDW may be formed over the slope region during summer. "Not quite bottom water" has also been observed off Wilkes Land, between 150 and 160°E (Foster, 1995) and has a similar pattern to the layer observed on this section.

On Legs 13 and 16 and to a lesser extent Leg 7 the neutral density surface 28.27 kg m^{-3} slopes up towards the shelf break more strongly than the other sections, and each of these legs has the coldest and freshest forms of the MCDW/AABW over the continental slope (Fig. 2). These three legs also have the strongest bottom intensification of westward flow based on the surface referenced velocities (Figs. 10a and b). The bottom intensification of the currents on these legs is consistent with dynamical models of dense water spilling over the continental slope, and in response

to Coriolis force turns westward along the slope and rise (Gill, 1973). This association between westward intensification of the bottom currents and extrema in local bottom water properties suggests that the large-scale thermo-haline structure over the slope is set by bottom-water-formation processes occurring nearby.

The overall evolution of the bottom-water properties for the more westerly sections shows that they are warmer and fresher (Fig. 2, Legs 11, 9, 7, 4 and 1). Given that the source of ADLBW is between 140 and 150°E and most likely from the Adelie Depression (Gordon and Tchernia, 1972; Rintoul, 1998), the bottom tracer distribution suggests that the bottom waters in this basin are spreading westwards along the continental rise. The consistency of the projected bottom velocities with the westward flow of tracers and buoy drifter tracks suggests that the choice of using the ADCP data for providing a reference velocity for the CTD data is valid.

The surface referenced velocity data have important implications for the ocean transport south of the SB and Antarctic Divergence. First, in the absence of any direct surface measurements, the best reference level to be used for calculating the interior ocean flow from the CTD data is the surface of the ocean, and not the bottom as is commonly used. Second, the surface velocities derived from the ADCP (and buoy) data suggest that there are significant transports associated with this depth-independent flow.

The circulation can be divided into baroclinic and barotropic components, defined respectively as the transport associated with the thermal wind field (referenced to the ocean surface) and the depth-independent part (Table 4). Because each meridional leg shows a distinctive change in sign from westward to eastward flow, we present the cumulative transport for both south and north of the point where the depth-integrated transport changes direction.

The westward barotropic component along the slope in the Australian-Antarctic Basin decreases from − 18 Sv at 94°E (Leg 4) to − 45 Sv at 128°E (Leg 13). The baroclinic component of the circulation is relatively small, and the barotropic

Table 4
The latitude where the westward flow becomes eastward, the barotropic, baroclinic and total transports south and north of the westward surface flow along each meridional leg. The baroclinic transport is the transport estimated using the CTD data and the ocean surface as the reference level. The barotropic transport is the transport derived from the ship based ADCP data. Negative means a westward transport. The units are Sv (10^6 m^3 s^{-1})

Leg	Latitude	Barotropic South	Baroclinic South	Total South	Barotropic North	Baroclinic North	Total North	Total Overall
1	− 65.11	− 9.5	− 6.5	− 16.0	5.1	− 11.4	− 6.4	− 22.4
4	− 64.46	− 18.2	0.4	− 17.7	6.1	− 0.1	5.9	− 11.8
7	− 64.08	− 24.0	− 4.4	− 28.4	18.0	− 8.5	9.6	− 18.9
9	− 65.09	− 30.6	0.4	− 30.1	49.9	− 8.7	41.1	11.0
11	− 65.43	− 28.3	− 1.0	− 29.3	− 8.4	− 9.2	− 17.7	− 46.9
13	− 64.25	− 45.5	− 9.9	− 55.4	4.7	− 16.7	− 12.0	− 67.4
16	− 65.4	− 8.5	− 1.4	− 9.9	40.2	− 21.9	18.3	8.4
18	− 64.8	− 39.5	− 9.1	− 48.6	20.2	− 12.7	7.6	− 41

circulation dominates the total westward transport. North of the westward flow the barotropic transport is eastwards, ranging from 5 to 50 Sv. The eastward transport is strongest in the western part of the survey between 100 and 120°E (on Legs 7 and 9), where the surface current suggests an eastward recirculation of the flow, and further east on Legs 16 and 18 where the eastward Antarctic Circumpolar Current (as represented by the SB) crosses these sections.

In the northern part where the surface flow is eastwards, all of these sections show a westward baroclinic transport (with the ocean surface as the reference level). On most legs (Legs 4, 7, 9, 16 and 18) the eastward barotropic transport is greater than the westward baroclinic transport to give an overall eastward transport. However, these barotropic transports are particularly sensitive to errors in the ADCP velocities. The rms error between the mapped ADCP velocities suggests that the barotropic transports could easily be in error by 6–12 Sv. However, the overall consistency of the westward surface velocities on all of the sections certainly suggests a strong slope and rise current with a barotropic, baroclinic and total westward transport (averaged over all sections) of -25, -3.9 and -29.4 Sv, respectively.

The large-scale circulation described here has some important implications for surface currents and surface water masses (Fig. 11). The 30 Sv westward current along the Antarctic slope and rise appears continuous from 95 to 150°E. Part of this slope current transports water through the Princess Elizabeth Trough (at 85°E) while some turns northward along Kerguelen Plateau (Leg 1) and then recirculates eastward south of the SB. This northward boundary current is consistent with a CTD section further to the north along the Kerguelen Plateau (Speer and Forbes, 1994) and joins another branch of the ACC that flows southeastward towards the Antarctic Continent. This second branch has a CDW that is marginally warmer and saltier than the warmest and saltiest CDW observed in the Princess Elizabeth Trough (Fig. 2, panels a and f). Evidence from the historical data and hydrographic sections along 140°E through the Australian-Antarctic Basin shows that a significant part of the second
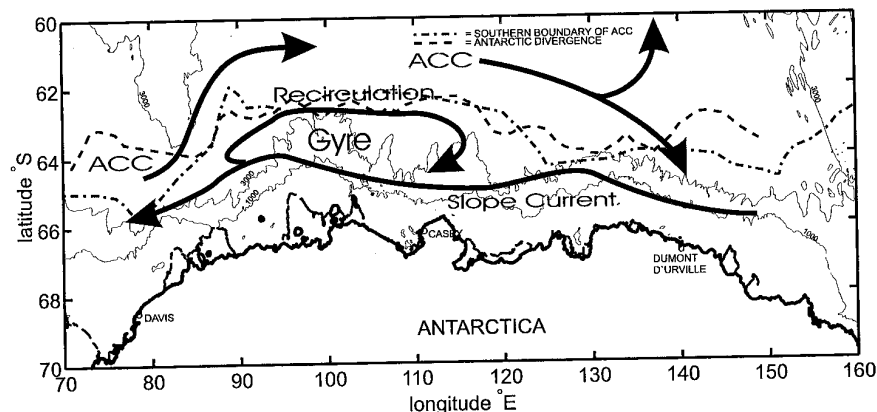

Fig. 11. A schematic diagram of the surface circulation of the BROKE survey region and the surrounding area based on the ADCP data, surface drifting buoys and water-mass properties.

branch turns northward again (Rintoul and Bullister, 1999), but some may turn west near 140–150°E as part of the westward slope current. However, more hydrographic data are needed to resolve this proposed circulation pattern for the eastern side of the survey region.

From these observations, and the position of the SB, it appears likely that the strong currents along the slope and the broad eastward flow in the western part of the survey region form a partially closed gyre. This partial gyre, although much smaller in areal size, is analogous to the Weddell gyre found in the Weddell-Enderby Basin, and the Ross Gyre found in the Ross and Bellingshausen Sea. The position of the SB, and the flow field and water-mass properties, suggest that this gyre is widest in the western part of the basin (near Legs 4, 7 and 9) and narrower in the eastern side (near Legs 16 and 18). This area is also the region where sea ice formed along the Antarctic continent coast is transported (Heil and Allison, 1999), consistent with this region having the widest sea-ice extent compared to the narrower part of the gyre between 135 and 150°E where the winter time sea-ice extent is a minimum (Gloersen et al., 1992).

Acknowledgements

References

Baines, P.G., Condie, S., 1998. Observations and Modelling of Antarctic Downslope Flows: A Review. In: Jacobs, S.S., Weiss, R.F. (Eds.), Ocean, Ice, and Atmsophere: Interactions at the Antarctic Continental Margin, Antarctic Research Series. American Geophysical Union, Washington, pp. 29–49.

Bindoff, N.L., Warner, M.J., Nicol, S., 1997. The Antarctic margin experiment. International WOCE Newsletter 26, 36–38.

Carmack, E.C., 1977. Water characteristics of the Southern Ocean south of the Polar Front. In: Angel, M. (Ed.), Voyage of Discovery: George Deacon 70th Anniversary Volume. Deep-Sea Research. Pergamon Press, Oxford, pp. 15–41.

Foldvik, A., Gammelsrod, T., Torreson, T., 1985. Circulation and water masses on the southern Weddell Sea shelf. In: Jacobs, S.S. (Ed.), Oceanonology of the Antarctic Continental Shelf, Antarctic Research Series. American Geophysical Union, Washington, pp. 5–20.

Foster, T.D., 1995. Abyssal water formation off the eastern Wilkes Land coast of Antarctica. Deep-Sea Research 42, 501–522.

Foster, T.D., Carmack, E.C., 1976. Frontal zone mixing and Antarctic Bottom Water formation in the southern Weddell Sea. Deep-Sea Research 23, 301–317.

Fukamachi, Y. et al., 2000. Seasonal variability of bottom water properties off Adelie Land, Antarctica. Journal Geophysical Research 105, 6531–6534.

Gill, A.E., 1973. Circulation and bottom water formation in the Weddell Sea. Deep-Sea Research 20, 111–140.

Gloersen, P. et al., 1992. Arctic and Antarctic sea ice, 1978–1987: satellite passive-microwave observations and analysis. National Aeronautics and Space Administration, Washington, Vol. SP-511, 290pp.

Gordon, A.L., Tchernia, P., 1972. Waters of the continental margin off Adelie coast, Antarctica. In: Hayes, D.E. (Ed.), Antarctic Research Series, Antarctic Oceanolgy II: The Australian–New Zealand Sector. American Geophysical Union, Washington, pp. 59–69.

Heil, P., Allison, I., 1999. The pattern and variability of Antarctic sea-ice drift in the Indian Ocean and Western Pacific sectors. Journal of Geophsical Research 104, 15789–15802.

Heywood, K.J., Locarnini, R.A., Frew, R.D., Dennis, P.F., King, B.A., 1998. Transport and water masses of the Antarctic Slope Front System in the Eastern Weddell Sea. In: Jacobs, S.S., Weiss, R.F. (Eds.), Ocean, Ice, and Atmosphere Interactions at the Antarctic Continental Margin, Antarctic Research Series. American Geophyscial Union, Washington, pp. 203–214.

Heywood, K.J., Sparrow, M.D., Brown, J., Dickson, R.R., 1999. Frontal sturctures and Anarctic Bottom Water flow through the Pricess Elizabeth Trough, Antarctica. Deep-Sea Research 46, 1181–1200.

Hoffman, E.E., Klinck, J.M., 1998. Thermohaline variability of the waters overlying the West Antarctic Peninsula continental shelf. In: Jacobs, S.S., Weiss, R.F. (Eds.), Ocean, Ice, and Atmosphere: Interactions at the Antarctic Continental Margin. American Geophysical Union, Washington, DC, pp. 67–81.

Jackett, D.R., McDougall, T.J., 1997. A neutral density variable for the world's ocean. Journal of Physical Oceanography 27 (2), 237–263.

Jacobs, S.S., Amos, A.F., Bruchhausen, P.M., 1970. Ross Sea Oceanography and Antarctic Bottom Water formation. Deep-Sea Research 17, 935–962.

Orsi, A.H., Johnson, G.C., Bullister, J.L., 1999. Circulation, mixing and production of Antarctic Bottom Water. Progress in Oceanography 43, 55–109.

Orsi, A.H., Whitworth III, T., Nowlin Jr., W.D., 1995. On the meridional extent and fronts of the Antarctic Circumpolar Current. Deep Sea-Research 42 (5), 641–673.

Rintoul, S.R., 1998. On the origin and influence of Adelie Land Bottom Water. In: Jacobs, S., Weiss, R. (Eds.), Ocean, Ice, and Atmosphere: Interactions at the Antarctic Continental Margin, Antarctic Research Series 75. American Geophysical Union, Washington, pp. 151–171.

Rintoul, S.R., Bullister, J.L., 1999. A late winter hydrographic section from Tasmania to Antarctica. Deep-Sea Research 46, 1417–1454.

Rodman, M., Gordon, A., 1982. Southern Ocean bottom water of the Australian-New Zealand sector. Journal of Geophysical Research 87, 5771–5778.

Rosenberg, M. et al., 1997. Aurora Australis marine science cruises AU9501, AU9604 and AU9601 — oceanographic field measurments and analysis, intercruise comparisons and data quality notes. Antarctic CRC, Hobart, Vol. 12, 150 pp.

Saunders, P.M., 1991. Calibration and standards. In: Joyce, T. (Ed.), WOCE Operations Manual. WHP Office, Wood Hole, pp. 1–11.

Speer, K., Forbes, A., 1994. A deep western boundary current in the South Indian Basin. Deep-Sea Research 41 (9), 1289–1303.

Tynan, C.T., 1998. Ecological importance of the Southern Boundary of the Antarctic Circumpolar Current. Nature 399, 708–710.

Wakatsuchi, M., Ohshima, K.I., Hishida, M., Naganobu, M., 1994. Observations of a street of cyclonic eddies in the Indian Ocean sector of the Antarctic Divergence. Journal of Geophysical Research 99 (C10), 20417–20426.

Whitworth III, T., Orsi, A.H., Kim, S.-J., Nowlin Jr., W.D., 1998. Water masses and mixing near the Antarctic Slope Front. In: Jacobs, S.S., Weiss, R.F. (Eds.), Ocean, Ice, and Atmsophere: Interactions at the Antarctic Continental Margin, Antarctic Research Series. American Geophysical Union, Washington, pp. 1–27.

Wong, P.S., Bindoff, N.L., Forbes, A., 1998. Ocean–ice shelf interaction and possible bottom water formation in Prydz Bay, Antarctica. In: Jacobs, S., Weiss, R. (Eds.), Ocean, Ice, and Atmosphere: Interactions at the Antarctic Continental Margin, Antarctic Research Series 75. American Geophysical Union, Washington, pp. 173–187.